DOI 10.7343/as-2025-852

ACQUE SOTTERRANEE
Italian Journal of Groundwater
journal homepage: https://www.acquesotterranee.net/

2025-AS53-852: 73 - 88

# Groundwater quality assessment using the Water Quality Index coupled with multivariate statistical analysis in the alluvial plains of El- Abd and El-That, Tiaret region, Northwestern Algeria

## *Valutazione della qualità delle acque sotterranee utilizzando l'Indice di Qualità dell'Acqua combinato con l'analisi statistica multivariata nelle pianure alluvionali di El-Abd e El-That, regione di Tiaret, Algeria nordoccidentale*

**ARDJANE Tedjeddine Adda**[a,b], **MEDDAH Boumediene**[a], **BEKKOUSSA Belkacem Samir**[c], **ZEMOUR Kamel**[b], **MAIRIF Mohamed**[b]

[a] Mustapha Stambouli University, Bioconversion Laboratory, Microbiology Engineering and Health Safety, Mascara, Algeria, email: *meddah19@yahoo.fr*
[b]Tissemsilt University, Institute of nature and life sciences, Algeria - email: *kamel.zemour@univ-tissemsilt.dz; Mairif.Mohamed@univ-tissemsilt.dz*
[c]cMustapha Stambouli University, Laboratory of Sciences and Technicals water, Mascara, Algeria - email: *b.bekkoussa@univ-mascara.dz*

**ARTICLE INFO**

Ricevuto/*Received*: 22 January 2025
Accettato/*Accepted*: 25 May 2025
Pubblicato online/*Published online*: 30 June 2025

**Handling Editor**:
**Chiara Sbarbati**

**Citation:**
Ardjane, T.A, Meddah, B., Bekkoussa, B.S., Zemour, K., Mairif, M. (2025). Groundwater quality assessment using the Water Quality Index coupled with multivariate statistical analysis in the alluvial plains of El- Abd and El-That, Tiaret region, Northwestern Algeria. Acque Sotterranee - *Italian Journal of Groundwater*, 14(2), 73 - 88
https://doi.org/10.7343/as-2025-852

**Correspondence to:**
**Ardjane Tedj Eddine Adda**
*tedjeddine.ardjane@univ-tissemsilt.dz*

**Keywords:**
*groundwater, water quality index, major ions, alluvial plains, hydrochemical-physical parameters.*

**Parole chiave:**
acque sotterranee, indice di qualità dell'acqua, ioni principali, pianure alluvionali, parametri idrochimico-fisico.



### *Abstract*

*Groundwater is considered as the living artery of each region worldwide. It is at the origin of such economic and agronomic development and help therefore to keep the local population in place especially in disadvantaged areas. This study assesses water quality index in the alluvial plains in northwestern region of Algeria. This index provides a value that expresses the overall water quality based on various parameters. Wherefore, field physical measurements coupled with laboratory hydrochemical analysis were used in this integrated study from 36 samples of three regions (Frenda, Ain Hedid and Takhemert). The obtained dominance of anions and cations in particular for* $HC0_3^-$ *,* $Cl^-$ *and* $Ca^{2+}$*,* $Mg^{2+}$ *highlighted that the chemical facies of the study area shown three facies. The first is bicarbonate calcium and the second is chloride sodium and the third one is bicarbonate magnesium. The high correlation of TDS (Total Dissolved Solids) with all ions notably* $Ca^{2+}$*,* $Mg^{2+}$*,* $Cl^-$ *,* $Na^+$ *except* $HC0_3^-$ *and* $N0_3^-$ *demonstrate that the mineralization, according to the literature, which is due to the alteration and dissolution of the source rock, in particular the carbonate rocks and the evaporitic rocks is the main factor of this correlation. For water quality index, the results showed that 2.77 % of the samples belong to the good quality category, while 63.88% and 33.33 % for poor and very poor quality respectively. Fortunately, the results of this index demonstrated the complete absence of unsuitable water quality. Nevertheless, given the vital importance of water and for the sustainable development of the region, the need to implement a continuous control of this source remains an urgent practice for the benefit of future generations.*

### Riassunto

L' acqua sotterranea è considerate l'arteria vitale di ogni regione del mondo. Questa è all'origine dello sviluppo economico e agronomico e contribuisce quindi a trattenere la popolazione locale sul posto, soprattutto nelle aree svantaggiate. Questo studio valuta l'indice di qualità dell'acqua nelle pianure alluvionali della regione nord-occidentale dell'Algeria. Questo indice fornisce un valore che esprime la qualità complessiva dell'acqua sulla base di diversi parametri. Pertanto, in questo studio integrato sono state utilizzate misure fisiche sul campo abbinate ad analisi idrochimiche di laboratorio su 36 campioni di tre regioni (Frenda, Ain Hedid e Takhemert). La dominanza ottenuta di anioni e cationi, in particolare per $HCO_3^-$, $Cl^-$ e $Ca^{2+}$, $Mg^{2+}$, ha evidenziato che la speciazione chimica dell'area di studio presenta tre facies. La prima bicarbonato-calcica, la seconda cloruro-sodica e la terza e bicarbonato-magnesiaca. L'elevata correlazione del TDS (Totale Solidi Disciolti) con tutti gli ioni, in particolare $Ca^{2+}$, $Mg^{2+}$, $Cl^-$, $Na^+$ eccetto $HCO_3^-$ e $NO_3^-$, dimostra che la mineralizzazione, anche in accordo con la letteratura, dovuta all'alterazione e alla dissoluzione della roccia madre, in particolare delle rocce carbonatiche e delle rocce evaporitiche, è il fattore determinante di questa correlazione. Per quanto riguarda l'indice di qualità dell'acqua, i risultati hanno mostrato che il 2.77% dei campioni appartiene alla categoria di buona qualità, mentre il 63.88% e il 33.33% appartengono rispettivamente alle categorie di qualità scarsa e molto scarsa. Fortunatamente, i risultati di questo indice hanno dimostrato la totale assenza di acque di qualità inutilizzabile. Tuttavia, data l'importanza vitale dell'acqua e per lo sviluppo sostenibile della regione, la necessità di implementare un controllo continuo di questa fonte rimane una questione urgente anche a beneficio delle generazioni future.

## Introduction

Groundwater is the main source that provides drinking water around the world (Jasechko et al., 2017). Also, it has an important resource for irrigation and industrial uses as well as hydropower generation and livestock production (El Baba et al., 2020). Unreliable rainfall frequently and quality water scarcity are serious concerns in many countries, especially in arid and semi-arid regions (Batarseh et al., 2021).

Studies on hydrochemical conditions aim to investigate and expend the knowledge on the hydrochemical pressures and impacts of natural processes and various human activities (Wątor & Zdechlik, 2021). The analysis of hydrochemical properties is intimately related to biological, physical, and chemical data for water quality (Mehreen et al., 2021). There are many natural factors that affect this quality, including hydrological, atmospheric, climatic, topographic and lithological factors (Galal Uddin et al., 2018). Recently, developing countries have serious problems in protecting water quality when attempting to improve water supply and sanitation (Galal Uddin et al., 2021).

Assessing water quality needs an analysis of large number of samples from many areas. The Water Quality Index (WQI) model is one of the tools developed to evaluate this characteristic (Galal Uddin et al., 2021, Misaghi et al., 2017). Many factors are responsible for the deterioration of water quality (Chadli & Boufala, 2021). This alteration can be detrimental to human health (Mehreen et al., 2021). Ameur et al. (2016) pointed up that in Tunisia the water quality is altered due to the nitrate pollution that originates from the excessive use of nitrate fertilizers. Same observations have been recorded in Morroco with a high value of 80.60 mg/L (Barakat, 2020). Therefore, to ensure the high water quality, it is necessary to evaluate it with the appropriate techniques (Li & Li, 2021 , Cosgrove et al., 2019).

In Algeria, studies on the quality of groundwater, particularly in the Northwestern zone, have held great importance through numerous studies (Zemour et al., 2023, Kenniche et al., 2022). Furthermore, this region is characterized by water scarcity and deteriorating water quality primarily due to climate change, particularly periods of intense drought, and secondarily due to human activities (Rahal et al., 2024). This study evaluates the current state of groundwater in the alluvial plains of El-Abd and El-Taht wadis in Tiaret. Given that people in these regions widely use groundwater resources for their own supply and agricultural needs, this study aims to provide a set of the quality of this resource.

The simple and traditional methods used in hydrochemical researches are essentially based only on a quantitative analysis of the physical-chemical parameters of groundwater. To better understand the origin and evolution model of groundwater, our study adopted different methods of analysis including the water quality index (WQI) assessment combined with Piper and Gibbs diagrams. In addition, multivariate statistical methods (PCA and HCA) were applied. Finally, the spatial distribution of the ions is used in this study.

## Materials and Methods

This study is carried out in the alluvial plains of El-Abd and El-That valley (Fig. 1) which are located in three regions of Tiaret province in Northwestern Algeria (Frenda, Ain Hedid and Takhemert). This study has swept an area of 44,630 km² between latitude 35°40' and 34°40' N and between longitudes 0°20' and 1°10' E. The alluvials plains are part of the sub-watershed of El-Abd and El-Taht valley, which belongs to the watershed of Mina valley. The latter belongs to the great basin of the Chellif valley (Fig. 3).

### *Geology and hydrogeological of the studied area*

The geological context of the wadis El- Abd and El-Taht consists of Upper Jurassic formations (Figure 2-1). These geological formations occupy the entire of El-Taht's watershed and half of the El- Abd's watershed (Safa, 2010). Also the Middle Jurassic and Callovo-Oxfordian formations largely predominate the other formations (Strojexport, 1976).

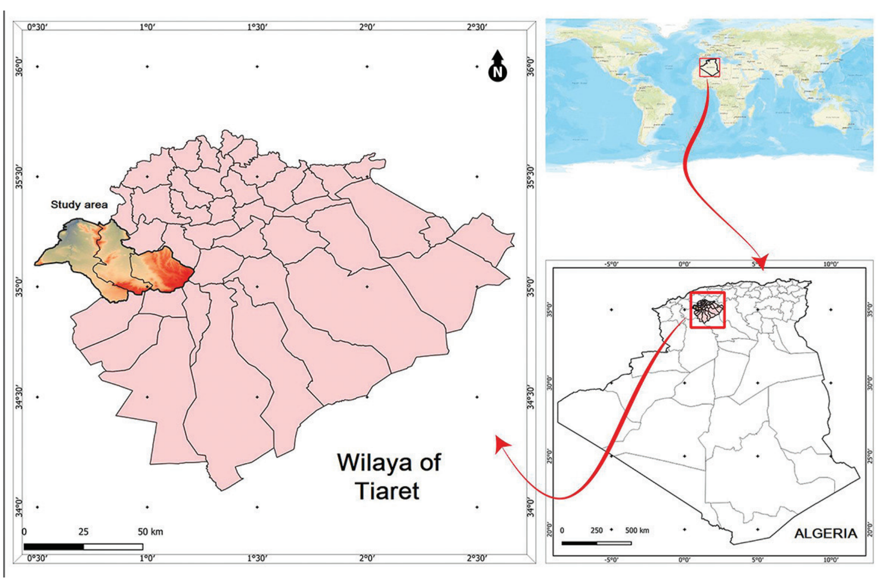


*Fig. 1 - Geographic localization of the studied area.*
Fig. 1 - Localizzazione geografica dell'area studiata.

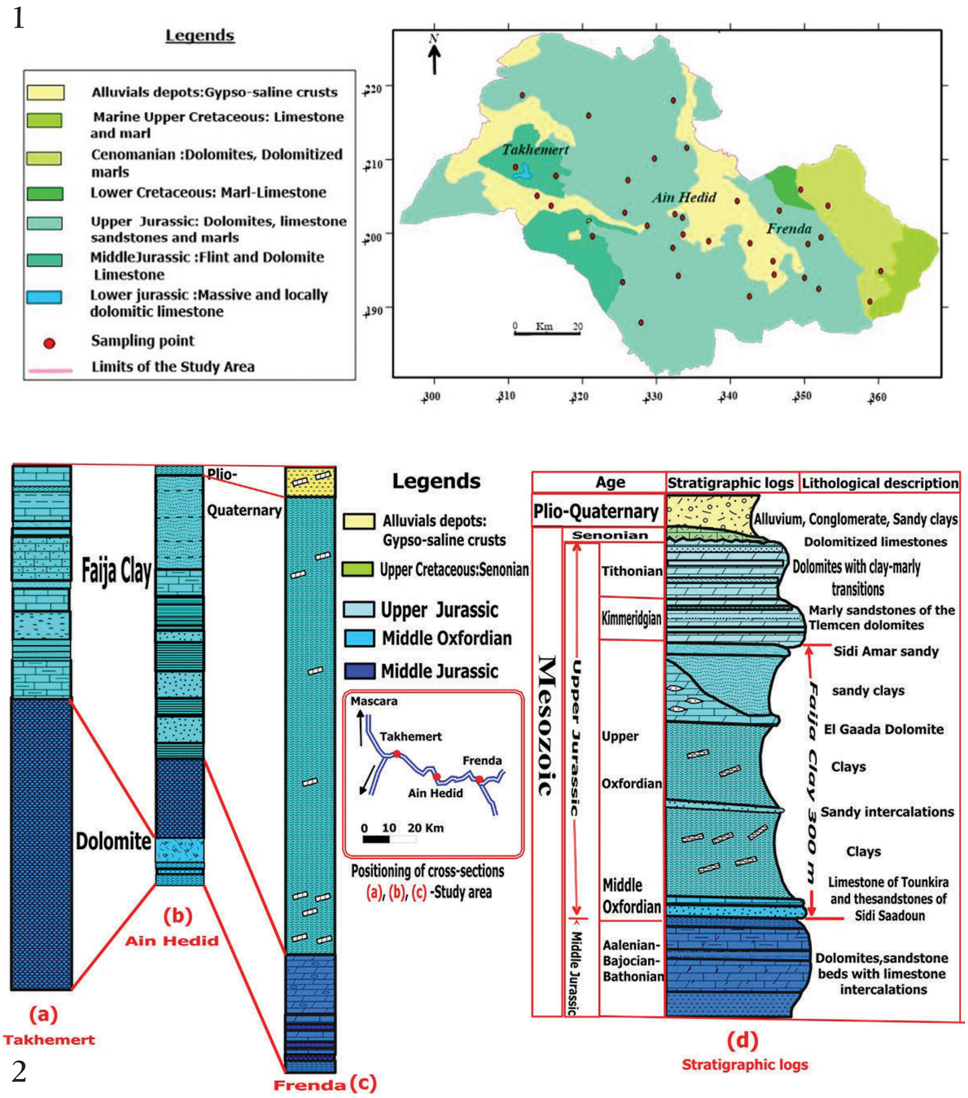


*Fig. 2 - Geological map (1) and stratigraphic logs (2) of the study area.*

Fig. 2 - Carta geologica (1) e colonne stratigrafiche (2) dell'area di studio.

To better understand the geology of the studied area, the stratigraphic logs located in Frenda, Ain Hedid, and Takhemert (Figs. 2a, 2b, 2c) show the vertical succession of the geological formations, particularly the variation in thickness of the El Gaada dolomites toward the south and southwest of the region. Additionally, Figure 2d highlights the thinning of the Upper Jurassic carbonate formations towards the northwest (Safa, 2010).

According to Figure 2d, two distinct hydrogeological environments are closely associated with the geological framework of the El-Taht watershed, the first one is in the downstream area, detrital formations consisting of clayey-loamy sands, pudding stones, and sandstone clays dominate, while the second one is in the upstream zone, carbonate formations prevail. In contrast, the El-Abd sub-watershed exhibits more significant surface runoff, influenced by the nature of its terrain and lithological structure.

The watersheds of the wadis El -That and wadis El-Abd have a complex hydrographic network, especially pronounced in their upstream regions, where they are fed by numerous karstic sources. In downstream, the density of the hydrographic network decreases due to the gentle slopes of the clay formations (Fig. 3).

According to Safa (2010), the El-Abd and El-Taht valleys have formed wide plains which are subject to erosion.

The alluvial plains are part of a vast hydrogeological system which is composed of three superimposed reservoirs. Firstly, the Plio-Quaternary formations (Figure 2,d), consist of clayey-loamy sands and massive limestone from the Senonian age, forming the base of a superficial aquifer. The second reservoir is made up of formations from the Portlandian and Kimméridgien periods, consisting of dolomitic formations with intercalations of sandstone and clay, which rest on an Oxfordian clayey substrate, representing a perched aquifer. The third reservoir is located in the fractured bedrock and constitutes the main deep reservoir of the region. It is characterized by the presence of dolomites, limestones, and sandstones from the Aaléno-Bajo-Bathonian age. At the top of this reservoir, there is a layer from the Callovo-Oxfordian age which is characterized by a thin and impermeable clay deposit with intercalations of sandstone and dolomite layers (Safa, 2010).

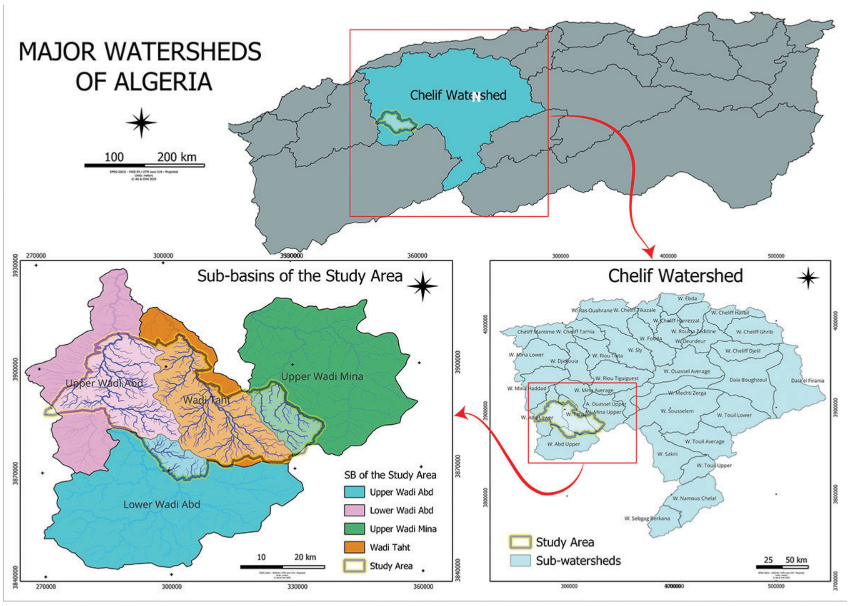


*Fig. 3 - Watershed localization of the study area.*

Fig. 3 - Localizzazione del bacino idrografico dell'area di studio.

Three superimposed aquifer levels are distinguished (Figure 2d):

1. A superficial aquifer within the Plio-Quaternary formations and Senonian limestone, with medium permeability.
2. A perched aquifer within the Kimmeridgian formations, resting on impermeable Oxfordian clays.
3. A deep aquifer within the fractured formations of the Aaléno-Bajo-Bathonian, confined beneath the Callovo-Oxfordian clays.

In order to better understand the hydrogeology of the alluvial plains as well as the dynamics and variations of groundwater in the two aquifers of the studied region, a piezometric map has been developed (Fig. 4).

According to this map, piezometric level varies among the three investigated areas. In Frenda, this level range from 689.5 to 1215.44 meters above sea level. As for Ain Hedid and Takhemert, the piezometric level varies between 564 and 950 meters above sea level, and between 526.8 and 728 meters above sea level respectively. Moreover, the Figure 5 highlights an information about the topography and elevation of the study area.

The Table 1 indicates additional information by specifying the geographical coordinates, static level and piezometric level of the 36 water points in the study area.

The static level was measured before the sampling of water intended for physico-chemical analyses at the beginning of June 2021. This operation was carried out over three days: the first day in the Frenda region, the second in Ain Hedid, and the third in Takhemert.

## Sampling procedures and analytical techniques

A total of 36 samples across the study area (Fig. 5) were collected between June to August (2021). All of them were

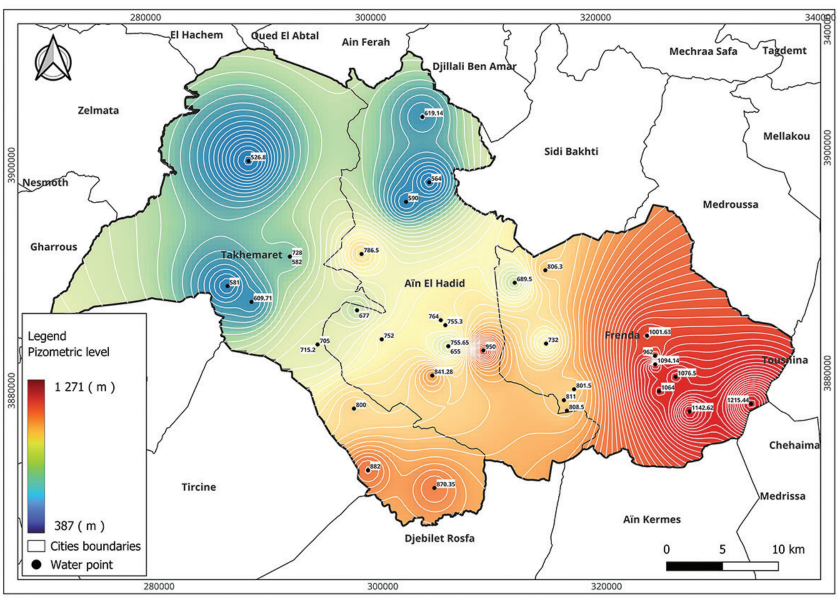


*Fig. 4 - Piezometric map of the study area (m asl).*

Fig. 4 - Carta piezometrica dell'area di studio (m slm).

*Tab. 1 - Geographic coordinates, static level and piezometric level of the sampling points in the study area.*
Tab. 1 - Coordinate geografiche, livello statico e quota piezometrica dei punti di campionamento nell'area di studio.

| Water point | Geographic coordinates | | Static level (m) | Elevation (m asl) | Piezometric level (m asl) |
|---|---|---|---|---|---|
| | X | Y | | | |
| F1 | 1.09798 | 35.04705 | 44.5 | 1121 | 1076.5 |
| F2 | 1.17174 | 35.02548 | 6.56 | 1222 | 1215.44 |
| F3 | 1.11158 | 35.01928 | 44.38 | 1187 | 1142.62 |
| F4 | 0.99155 | 35.01995 | 44.5 | 853 | 808.5 |
| A1 | 0.87556 | 35.07156 | 32.35 | 788 | 755.65 |
| A2 | 0.78325 | 35.02164 | 45 | 845 | 800 |
| A3 | 0.85021 | 35.25491 | 8.86 | 628 | 619.14 |
| A4 | 0.85992 | 35.0481 | 8.72 | 850 | 841.28 |
| T1 | 0.68299942 | 35.1070021 | 26.29 | 636 | 609.71 |
| T2 | 0.68015797 | 35.2196824 | 18.2 | 545 | 526.8 |
| A5 | 0.86823 | 35.09242 | 34 | 798 | 764 |
| A6 | 0.81044 | 35.07708 | 91 | 843 | 752 |
| A7 | 0.87556 | 35.07156 | 133 | 788 | 655 |
| A8 | 0.86199 | 34.95796 | 66.65 | 937 | 870.35 |
| F5 | 0.97052 | 35.13237 | 66.7 | 873 | 806.3 |
| F6 | 1.06979 | 35.08003 | 59.37 | 1061 | 1001.63 |
| F7 | 1.0778 | 35.06391 | 133 | 1095 | 962 |
| F8 | 1.07798 | 35.05705 | 8.86 | 1103 | 1094.14 |
| T3 | 0.79703017 | 34.9722646 | 45 | 927 | 882 |
| T4 | 0.74769372 | 35.0729593 | 26.8 | 742 | 715.2 |
| T5 | 0.74769481 | 35.0729142 | 40 | 745 | 705 |
| T6 | 0.65963236 | 35.1196789 | 30 | 611 | 581 |
| T7 | 0.72061761 | 35.1433479 | 60 | 788 | 728 |
| T8 | 0.72051008 | 35.143256 | 68 | 650 | 582 |
| F9 | 1.08174 | 35.03548 | 83 | 1147 | 1064 |
| F10 | 0.98863 | 35.0283 | 28 | 839 | 811 |
| F11 | 0.99858 | 35.0371 | 48.5 | 850 | 801.5 |
| F12 | 0.94052 | 35.12237 | 65.5 | 755 | 689.5 |
| F13 | 0.97121 | 35.07367 | 50 | 782 | 732 |
| F 14 | 0.98863 | 35.02839 | 44.5 | 839 | 794.5 |
| A9 | 0.8727 | 35.08843 | 37.7 | 793 | 755.3 |
| A10 | 0.79072 | 35.14535 | 34.5 | 821 | 786.5 |
| A11 | 0.83421 | 35.18703 | 87 | 677 | 590 |
| A12 | 0.85691 | 35.20271 | 81 | 645 | 564 |
| A13 | 0.7863 | 35.10032 | 98 | 775 | 677 |
| A14 | 0.90991 | 35.06826 | 40 | 990 | 950 |

collected in pre-cleaned polyethylene bottles with high quality. Our sampling method was based on a selection of 36 wells during low flow, taking into account the location of water sources in relation to the lithology of the study area. The samples were taken after pumping for 10 to 15 min until constant conductivity, were kept in coolers (at 4 C°) until physical-chemical laboratory analyses.

In this study, the quantification of anions and cations is useful for identifying the ionic composition of the water, which is essential for assessing its mineralization and detecting possible pollution. The Water Quality Index (WQI) aims to provide a global and synthetic assessment of water quality based on several physicochemical parameters. A complementary study to classify water types according to their dominant ionic composition (Piper diagram) and identify the major geochemical processes controlling water composition (Gibbs diagram) will be conducted.

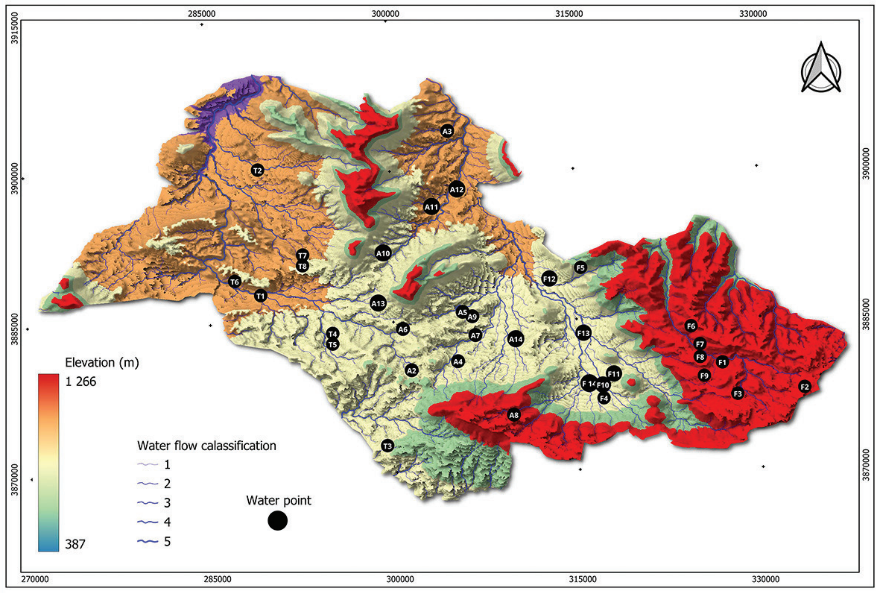


*Fig. 5 - Location of water point in the study aera.*

Fig. 5 - Ubicazione dei punti di campionamento delle acque nell'area di studio.

Consequently, 17 parameters were analyzed in situ[1] and in the laboratory[2] according to Rodier et al. (2009). [1]Conductivity (EC), (pH), water temperature (T°) and (TDS) were measured using a portable device (HACH SL 1000). The instrument was calibrated using buffer solutions with pH values of 4, 7 and 9, as well as EC values of 147, 1413, and 12.88 µS/cm, respectively.[2]The concentration of calcium ($Ca^{2+}$), magnesium ($Mg^{2+}$), chloride ($Cl^-$) and bicarbonate ($HCO_3^-$) was determined by the volumetric method. The EDTA titration analysis was used to examine calcium using Eriochrome Black and Murexide indicators, respectively. The nitrates ($NO_3^-$) and sulfate ($SO_4^{2-}$) were measured using a Spectrophotometer (HACH DR2500).

For the sodium and potassium, the concentration was determined using flame photometer (Jenway PFP7). Methyl orange was used with HCl (0.1N) titration to determine the bicarbonate ($HCO_3^-$). Chloride ($Cl^-$) was determined by titrating with silver nitrate ($AgNO_3^-$) solution using potassium chromate ($K_2CrO_4$).

The error ionic balance (EIB) has been assessed in this study to confirm the analytical precision for correct ion measurement. Several studies have established this EIB on a value precision at approximately ±8% (Fu et al., 2022) and ±10% (El Baba et al., 2020). However in our study this error ionic balance is acceptable at ± 5% (Adimalla, 2019, Adimalla and Qian, 2021) using following equation:

EIB=(∑ Cations - ∑ Anions) / (∑ Cations + ∑ Anions)·100

### *Water quality index (WQI)*

In order to properly classify water quality according to international standards as recommended by the WHO (2008), a quality index has been adopted in this study (Vasanthavigar et al., 2010). This index provides the composite influence of individual parameters on the overall quality of water for human consumption.

This index is calculated using the following equation reported by Bekkoussa et al., (2017):

Step 1

$$WQI = \sum SI_i = \sum W_i q_i = \sum \left[ \left( \frac{w_i}{\sum_{n}^{i=1} w_i} \right) \cdot \left( \frac{C_i}{S_i} \cdot 100 \right) \right] \qquad (1)$$

Where:

$C_i$: concentration of each parameter,
$S_i$: limit value of each parameter set by WHO standards,
$w_i$: the weight of each parameter according to its relative importance in the quality of drinking water (Table 2),
$q_i$: quality notation for each parameter,
$W_i$: the relative weight,
$SI_i$: the sub-index of parameteri.

*Tab. 2 - Weight of physico-chemicals parameters (Bekkoussa et al., 2018).*

Tab. 2 - Peso dei parametri fisico-chimici (Bekkoussa et al., 2018).

| Parameters | Si (WHO standard maximum value) 2008 | $w_i$ | $W_i$ |
|---|---|---|---|
| pH | 9 | 3 | 0.094 |
| TDS(ppm) | 1500 | 5 | 0.156 |
| $Cl^-$(mg/L) | 250 | 4 | 0.125 |
| $SO_4^{-2}$ (mg/L) | 250 | 4 | 0.125 |
| $Ca^{2+}$(mg/L) | 100 | 2 | 0.063 |
| $Na^+$(mg/L) | 150 | 3 | 0.094 |
| $K^+$(mg/L) | 12 | 3 | 0.094 |
| $Mg^{2+}$ (mg/L) | 50 | 2 | 0.063 |
| $HCO_3^-$(mg/L) | 250 | 1 | 0.031 |
| $NO_3^-$(mg/L) | 50 | 5 | 0.156 |
| **Total** | | **32** | **1** |

For a detailed explanation of the applied calculations, a numerical value named relative weight ($W_i$), specific to each physico-chemical parameter is calculated using following Equation according to Brown (Brown et al.,1970,1972):

$$W_i=K/S_i \quad (2)$$

Where:

K: proportionality constant and is calculated using the following equation:

$$K = 1/\sum^{n}_{i=1}\left(1/S_i\right) \quad (3)$$

n: number of parameters

$S_i$: maximum value of the WHO standard (2008) for surface water of each parameter in mg/L except for pH and TDS (ppm).

Step 2: the sub-index ($SI_i$) value was calculated by using the expression

$$SI_i = \left[\left(C_i - S_o\right)\right] / \left[\left(S_i - S_o\right)\right] \cdot 100 \quad (4)$$

where

$S_o$ = actual values of the parameters in pure water (generally $S_o$ = 0 for most parameters, except for pH).

$S_{pH}$ = {(C pH − 7)} / {(8.5 − 7)} × 100

### Irrigation index

In this study, a set of parameters such as the sodium adsorption ratio (Richards, 1954), sodium percentage (Wilcox, 1955), Kelly's ratio (Kelly, 1963) and magnesium hazard ratio (Ragunath, 1987) were evaluated to determine the irrigation index of the groundwater in the studied area, using the following equations:

$$SAR = \frac{Na}{\sqrt{\frac{Ca+Mg}{2}}} \quad (a)$$

$$Na\% = \frac{Na+K}{Ca+Mg+Na+K} \cdot 100 \quad (b)$$

$$KI = \frac{Na}{\left(Ca+Mg\right)} \quad (c)$$

$$MH = \frac{Na}{\left(Ca+Mg\right)} \cdot 100 \quad (d)$$

### Statistical analysis

Various statistical techniques including PCA and HCA are used to present our data using SPSS 20 software and OriginoPro 22. PCA is one of the important statistical methods that groups the data based on the inter-correlations between the variables and similarity between study factors. Correlations between water quality variables can mention many significant hydrochemical relationships (Adimalla & Qian, 2021). The box plots have been set up using OriginoPro 22.

## Hydrochemical Characteristics of groundwater of the study area

### Hydrochemical Composition

All charge-balance errors (EIB) for the three regions are within an acceptable limit of ±5%. The groundwater of the study area is characterized by its richness in the chemical elements. The results of the surveyed water chemical and physical parameters are shown in Table 3.

As expected, for all samples the pH values have alkaline properties. Previous studies indicated the alkaline nature of the groundwater in Algeria (El Baba et al., 2020, Zemour et al., 2023).

The Piper diagram (Fig. 6) illustrates three distinct chemical facies: the first facies is $HCO_3$-Ca (27.77%), the second facies is Cl-Na (25%), and the third facies is $HCO_3^-$Mg (19.44%). This could be explained by the increase in $Ca^{2+}$ and $Mg^{2+}$ concentrations resulting from the dissolution of carbonate formations (calcite and dolomite), as well as the dissolution of evaporitic formations (halite), which leads to a rise

*Tab. 3 - Groundwater Physicochemical parameters.*

Tab. 3 - Parametri fisico-chimici delle acque sotterranee.

| Components | FRENDA | | | AIN HEDID | | | TAKHEMERT | | |
|---|---|---|---|---|---|---|---|---|---|
| | Min | Max | Mean | Min | Max | Mean | Min | Max | Mean |
| $Na^+$ (mg/L) | 22 | 265 | 61.51 | 29 | 415 | 185 | 24 | 225 | 129.75 |
| $Ca^{2+}$ (mg/L) | 48.89 | 142.68 | 100.31 | 44.08 | 226.8 | 136.79 | 48.89 | 195.59 | 135.06 |
| $Mg^{2+}$ (mg/L) | 3.96 | 103.66 | 47.69 | 30.25 | 160.704 | 78.12 | 4.96 | 202.36 | 59.02 |
| $K^+$ (mg/L) | 1.2 | 13.8 | 5.99 | 2.4 | 19.4 | 9.43 | 2.5 | 8.5 | 4.11 |
| $HCO_3^-$ (mg/L) | 201.3 | 463.6 | 358.16 | 262.3 | 463.6 | 345.96 | 323.3 | 463.6 | 366 |
| $SO_4^{-2}$ (mg/L) | 12.9 | 219.11 | 84.71 | 20.14 | 466.75 | 191.21 | 13.7 | 193.07 | 128.59 |
| $Cl^-$ (mg/L) | 56.8 | 383.4 | 126.28 | 71 | 937.2 | 377.3 | 35.5 | 454.4 | 284 |
| $NO_3^-$ (mg/L) | 3.53 | 141.71 | 66.45 | 4.33 | 152.95 | 34.66 | 14.49 | 117.87 | 53.05 |
| T° C° | 26 | 29 | 27.89 | 25.3 | 29.2 | 27.56 | 25.5 | 29.2 | 27.6 |
| pH | 7.4 | 7.63 | 7.55 | 7.25 | 7.83 | 7.55 | 7.27 | 7.82 | 7.41 |
| EC (µS/cm) | 477 | 1860 | 1097.79 | 765 | 4630 | 2047.7 | 615 | 2390 | 1614.8 |
| TDS (ppm) | 239 | 933 | 549.5 | 383 | 2320 | 1038.64 | 308 | 1194 | 807.37 |

in $Cl^-$ and $Na^+$ concentrations in the water. Moreover, the study area, located 200 km from the sea, suggests the absence of $Na^{+2}$ and $Cl^-$ intrusion into the groundwater.

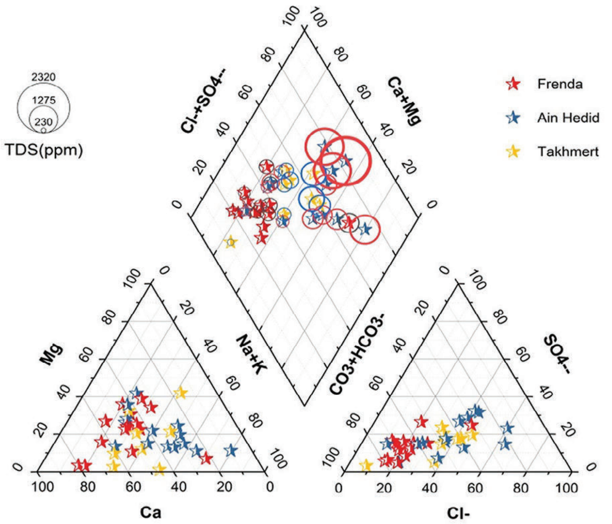


*Fig. 6 - Piper diagram.*

Fig. 6 - Diagramma di Piper.

Indeed, according to average results, among the measured element $Ca^{2+}$ (6.10 meq/L) and $Mg^{2+}$ (5.10 meq/L) represent the majority cation, while chloride (7.30 meq/L) is the most dominant anion. This could be explained by the dissolution of $Ca^{2+}$, $Mg^{2+}$ and $Cl^-$ with respect from calcite, dolomite and Halite (Chen et al., 2023; Martínez-Martínez et al., 2021).

This richness in $Ca^{2+}$ is significantly observed in Ain Hedid (226.8 mg/L), a value that exceed the drinking water standard of 75 mg/L (WHO, 2008). Indeed, this same region (Ain Hedid) recorded the highest value of $Cl^-$ (Table 3). In another study carried out in the Ghriss plain basin (Western Algeria), Bekkousa et al. (2017) demonstrated the same findings.

The result showed that the study area has a high $NO_3^-$ and EC value exceeding WHO standards (2008). The use of fertilizers and pesticides in agricultural practice could be the main factor contributing to the increase for $NO_3^-$ levels. Our study externalizes results exceeding those reported by Kenniche et al. (2022) in the Ghriss plain basin (Western Algeria).

According to the spatial distribution of ions, calcium is distributed over the entire plain with high concentrations and above the standard (WHO, 2008) with a maximum value of 226.8 mg/L. Both of the magnesium and sodium are strongly localized in the north and south west of Ain Hedid and the center of Takhemert (Figs 7e, 7d), with 160.704 (mg/L) 202.36 (mg/L) respectively.

The majority ions, including chloride with a maximum value of 454.4 mg/L, exceeded the WHO standard (2008) and are generally distributed in the Northwestern part of Ain El Hedid. Additionally, high nitrate concentrations are found in the northwestern part of Ain El Hedid (152.95 mg/L) and the center of Frenda (141.71 mg/L) (Fig. 7c).

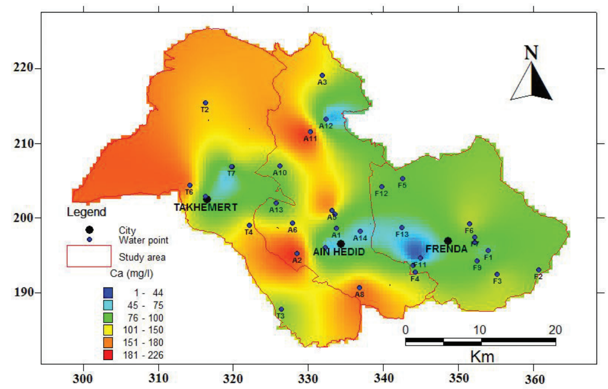


*Fig. 7a - Spatial distribution of $Ca^{2+}$ in the study area.*

Fig. 7a - Distribuzione spaziale del $Ca^{2+}$ nell'area di studio.

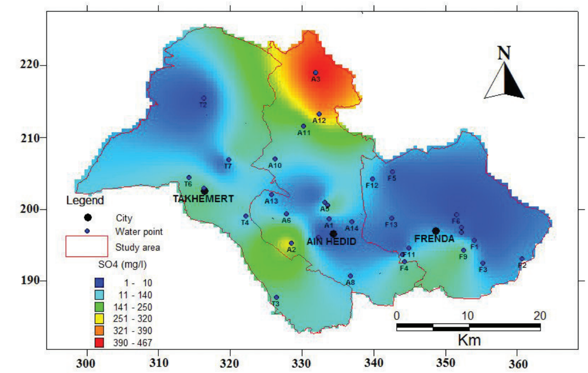


*Fig. 7b - Spatial distribution of $SO_4^{2-}$ in the study area.*

Fig. 7b - Distribuzione spaziale di $SO_4^{2-}$ nell'area di studio.

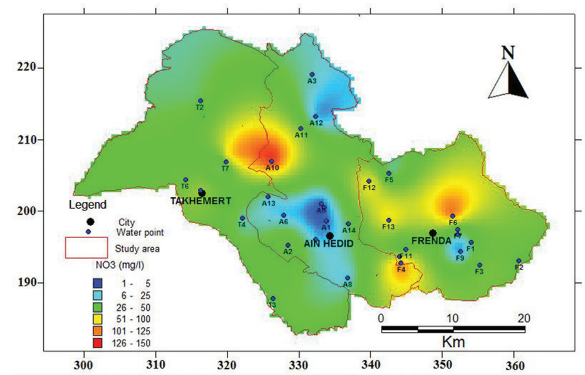


*Fig. 7c - Spatial distribution of $NO_3^-$ in the study area.*

Fig. 7c - Distribuzione spaziale di $NO_3^-$ nell'area di studio.

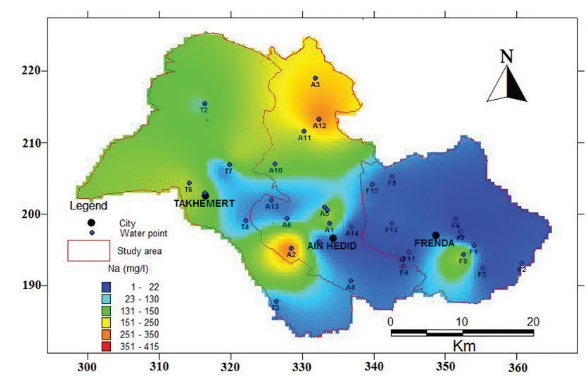


*Fig. 7d - Spatial distribution of $Na^{2+}$ in the study area.*

Fig. 7d - Distribuzione spaziale di $Na^{2+}$ nell'area di studio.

*Fig. 7 - Spatial distribution of the major cations and anions in the study area.*

Fig. 7 - Distribuzione spaziale dei principali cationi e anioni nell'area di studio.

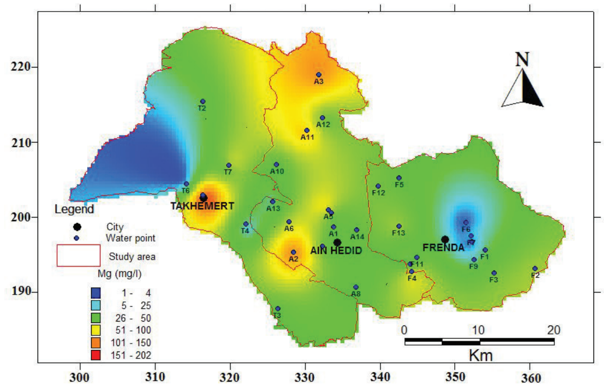


*Fig. 7e - Spatial distribution of $Mg^{2+}$ in the study area.*

Fig. 7e - Distribuzione spaziale del $Mg^{2+}$ nell'area di studio.

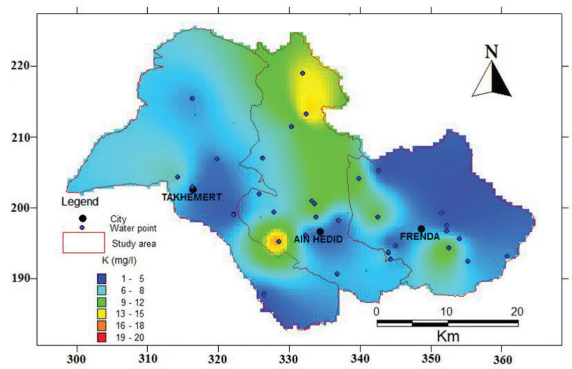


*Fig. 7f - Spatial distribution of $K^+$ in the study area.*

Fig. 7f - Distribuzione spaziale di $K^+$ nell'area di studio.

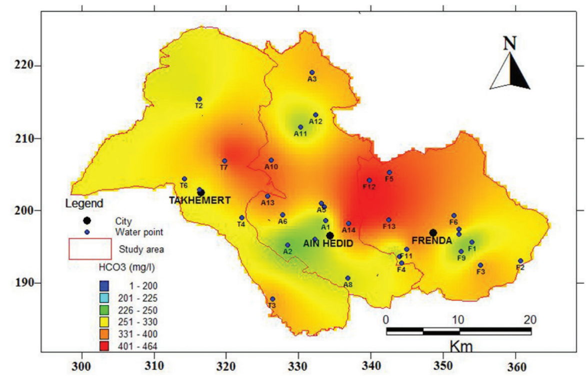


*Fig. 7g - Spatial distribution of $HCO_3^-$ in the study area.*

Fig. 7g - Distribuzione spaziale di $HCO_3^-$ nell'area di studio.

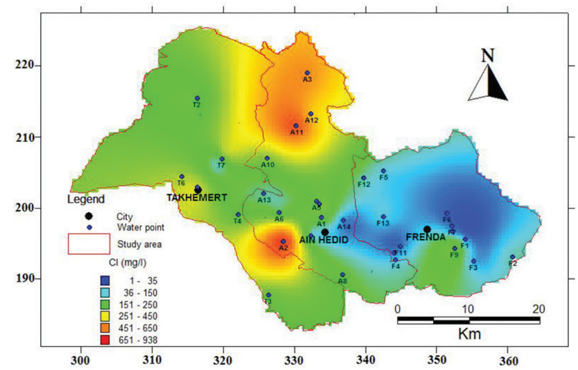


*Fig. 7h - Spatial distribution of $Cl^-$ in the study area.*

Fig. 7h - Distribuzione spaziale di $Cl^-$ nell'area di studio.

### *Major ion correlation*

Correlation analysis helps assess the relationships between the hydrochemical parameters of groundwater (Cosgrove et al., 2019). Electrical conductivity (EC) shown a strong positive correlation with most ions, except for $HCO_3^-$ and $NO_3^-$ (Fig. 8). The correlations with $Cl^-$, $SO_4^{2-}$, and $Na^+$ are all greater than 0.8. Fu et al. (2022) showed that EC is largely influenced by these ions.

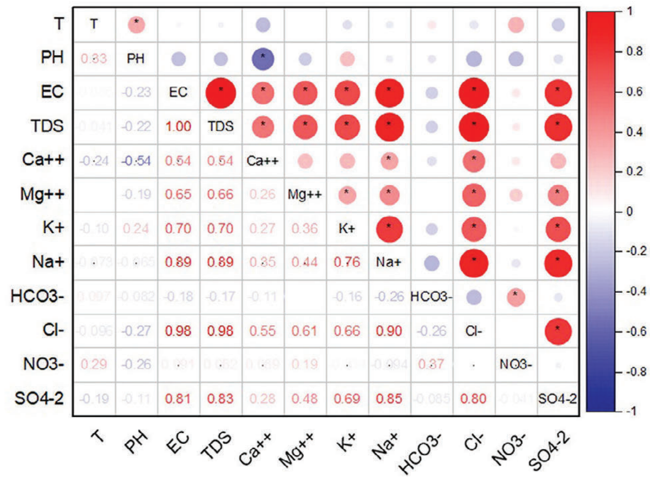


*Fig. 8 - Correlation between groundwater hydrochemical parameters of the studied area.*

Fig. 8 - Correlazione tra i parametri idrochimici delle acque sotterranee dell'area studiata.

The correlation between pH and other elements is relatively weak, a similar pattern being observed for $HCO_3^-$ and $NO_3^-$. Our results also indicated a positive correlation between $Na^+$ and $Cl^-$, likely due to the dissolution of evaporitic minerals such as halite and gypsum (Calligaris et al., 2019). Additionally, we observed a positive correlation between $Na^+$ and $SO_4^{2-}$, which can be attributed to the dissolution of Glauber's salt ($Na_2SO_4{\cdot}10H_2O$), a common source of both ions. Certain clay minerals, particularly illites, may incorporate sodium and potassium cations in their structure, explaining the positive correlation between $Na^+$ and $K^+$ (Kom et al., 2023). We also found a positive correlation between Cl– and $K^+$, linked to the dissolution of evaporitic minerals like sylvite. Furthermore, $Cl^-$ has a strong positive correlation with $SO_4^{2-}$ and $Mg^{2+}$, likely due to groundwater interacting with geological formations, releasing these ions into the water through natural geochemical processes or human activities.

### *Evolution of Groundwater Chemistry*

Gibbs diagram provides a method for better understanding the processes that affect geochemical parameters underlying groundwater mineralization (Yahiaoui et al., 2023). It is intended to study the essential natural mechanisms controlling water chemistry and also to establish the relationship between the water composition and the lithological characteristics of the aquifer. Precipitation effects, rock weathering, and evaporation are the main factors involved in this diagram (Gibbs, 1970). According to Figure 9, evaporation and mineral

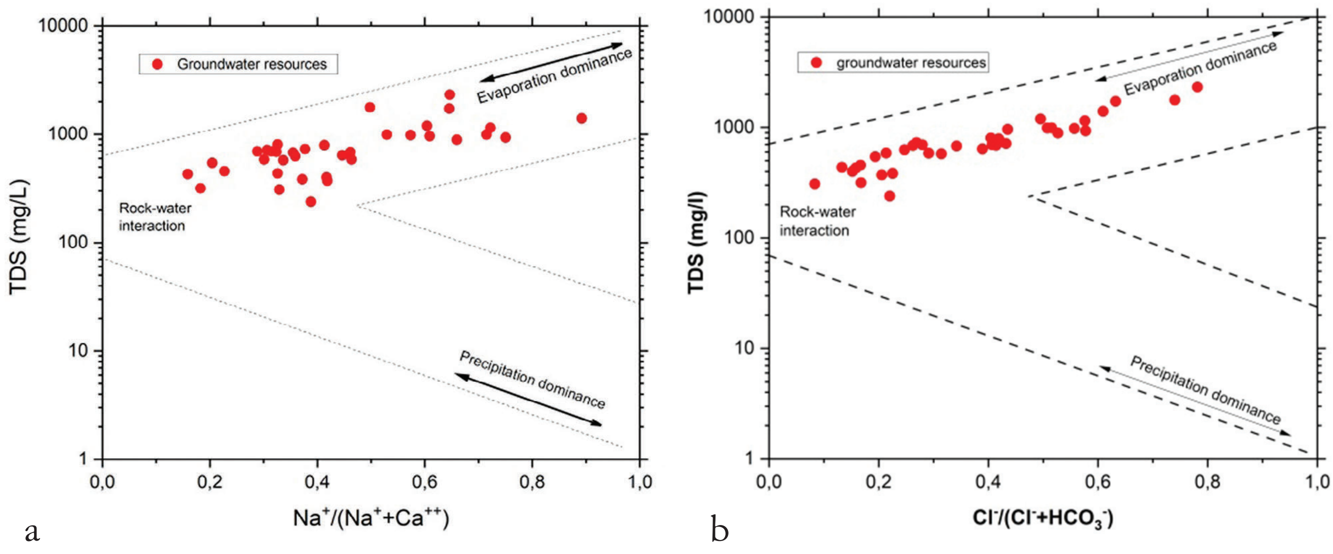


*Fig. 9 - Gibbs diagram.*
Fig. 9 - Diagramma di Gibbs.

weathering are the main factors affecting the chemical composition of studied groundwater.

### Classification of water according to the Durov Diagram

The Durov diagram is based on the percentage of major ions in meq/L (Durov, 1948), where the percentages of total positive and negative ions always add up to 100%. The values of cations are represented in the left triangle, while those of anions are located in the upper triangle. Both are then projected onto the main field square. This diagram has the advantage of visualizing various geochemical processes that could influence water formation. Lloyd and Heathcoat (1985) divided the central square into nine sectors, each representing a specific hydrochemical process.

The Durov diagram (Fig. 10) can explain three major processes: mixing/dissolution, ion exchange, and reverse ion exchange, especially when the total water concentration exceeds 1500 mg/L. This method was adopted to assess water types based on geochemical processes that may have influenced the nature of groundwater. It also allows presenting total concentrations of cations and ions, as well as pH and TDS.

The diagram results shown that most water samples exhibit simple dissolution or mixing. The results corroborate those obtained by the Gibbs diagram (Fig. 9).

### Statistical analysis with PCA (Principal Component Analysis) and (HCA) (Hierarchical Cluster Analysis)

For more characterizing the revealed water parameters, the Principal component analysis (PCA) is adopted by previous studies (Gibbs, 1970; Gaur et al., 2022; Rahman et al., 2021; Adimalla, 2019, Gan et al., 2022).Therefore, the Scree plot has been, generally, using for selecting the principal components

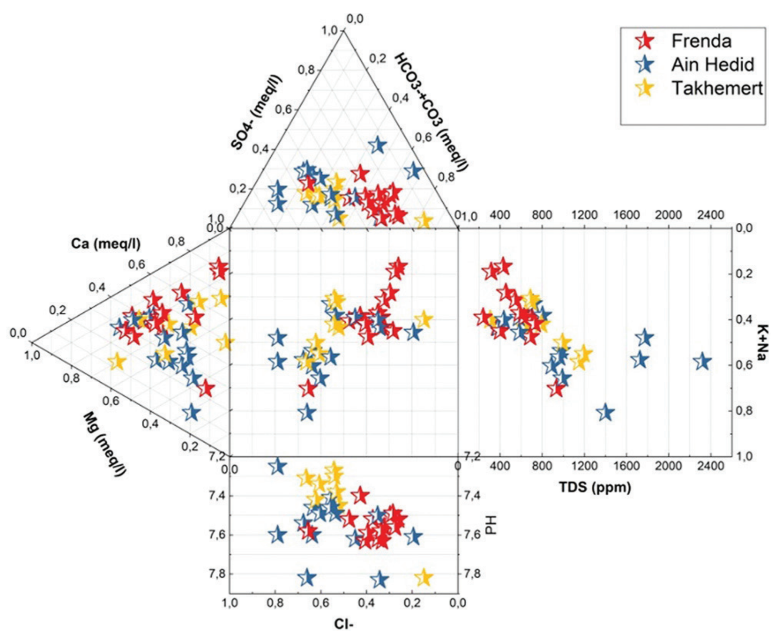

*Fig. 10 - Durov Diagrams.*
Fig. 10 - Diagrammi di Durov.

(PCs) (Fartas et al., 2022). Figure 11 highlighted that the first three components have the highest contribution to explain the variance of 49.14%, 14.66% and 12.755%. Hence, they accounted for 76.553% of the variability within the data.

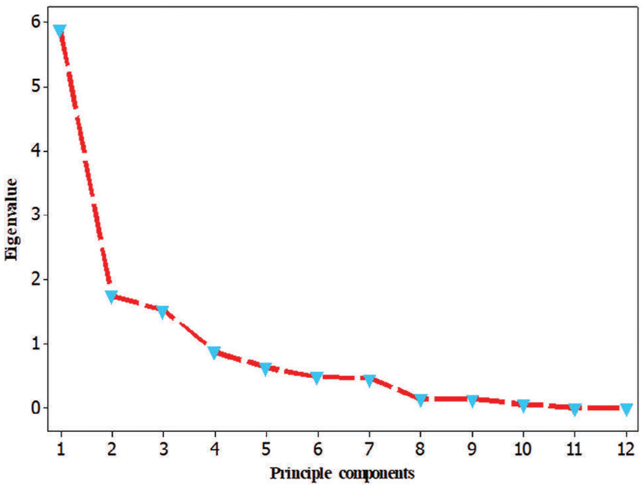


*Fig. 11 - Principle component analysis (PCA) screen plot of studied parameters.*
Fig. 11 - Diagramma dell'analisi delle componenti principali (PCA) dei parametri studiati.

Table 4 shows the factor weights values of observed factors related to each principal component. The coefficients of each parameter indicated the contribution of the corresponding variable to the specific principal component. Previously, Liun et al. (2003) have given the classification of PCs according to these values. Indeed the PCs are classed as weak, moderate, and strong if their factor loading values are 0.30–0.50, 0.50–0.75, and > 0.75 respectively.

*Tab. 4 - Principal component loadings of the PCA.*
Tab. 4 - Carichi delle componenti principali della PCA.

| | PC1 | PC2 | PC3 |
|---|---|---|---|
| T°C | -0.019 | 0.555 | 0.555 |
| pH | -0.064 | 0.916 | -0.160 |
| EC | 0.971 | -0.169 | 0.066 |
| TDS | 0.975 | -0.163 | 0.063 |
| $Ca^{2+}$ | 0.430 | -0.690 | -0.023 |
| $Mg^{2+}$ | 0.641 | -0.136 | 0.318 |
| $K^+$ | 0.811 | 0.234 | -0.132 |
| $Na^+$ | 0.937 | 0.023 | -0.149 |
| $HCO_3^-$ | -0.215 | -0.058 | 0.647 |
| $Cl^-$ | 0.951 | -0.218 | -0.040 |
| $NO_3^-$ | 0.024 | -0.160 | 0.843 |
| $SO_4^{2-}$ | 0.872 | -0.033 | -0.075 |

It was determined that the PC1 was connected with a positive weight with, conductivity (0.971), sodium (0.937), chloride (0.951), potassium (0.811), and $SO_4^-$ (0.872) with 49.14 per cent variation. This group of variables associated with PC1 indicates that salinization is the main factor influencing mineralization. Thus, the increase in salinity is primarily linked to the dissolution of minerals and the weathering of evaporitic rocks (Benadela et al .,2022). The second factor PC2, representing 14.66% of the total variance, is strongly correlated with pH (0.916) and T°C (0.555), suggesting that the increase in temperature influences the rate of chemical reactions, potentially leading to a rise in the pH of the waters (BITENCOURT et al., 2019). However, Nitrate (0.843) and $HCO_3^-$ (0.647) had positive weight in PC3, with a 12.76% of variance (Fig. 12). These elements are the main indicators of contamination related to agricultural activities (Bekkoussa et al., 2018).

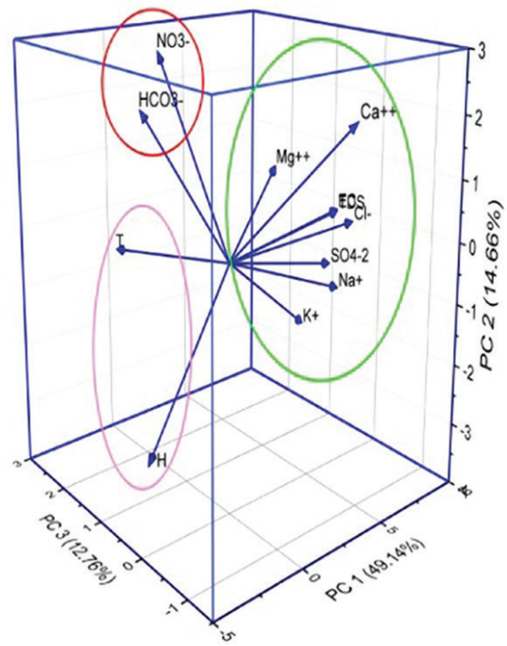


*Fig. 12 - Component diagram (PCA).*
Fig. 12 - Diagramma delle componenti (PCA).

The HCA method is the most approach which uses squared Euclidean distance that gives the most meaningful findings (Sharma et al., 2017). Cluster analysis using Ward's method and squared Euclidean distance (Fig. 13) validated the results of the Piper diagram (Amadou et al., 2022). The water sources are grouped into three main categories:

Cluster (A) (22.22% of sources): Primarily controls the salinity of groundwater, with a major influence from $Na^+$ and $Cl^-$ resulting from the dissolution of evaporitic formations (halite).

Cluster (B) (25% of sources): Includes $HCO_3^-$, $Ca^{2+}$, and $Mg^{2+}$, highlighting the role of the dissolution of carbonate rocks (limestone, dolomite) and evaporitic minerals (gypsum) in groundwater chemistry.

Cluster (C): Dominated by the dissolution of dolomite [$CaMg(CO_3)_2$], representing the majority of sources in the region (52.77% of sources)

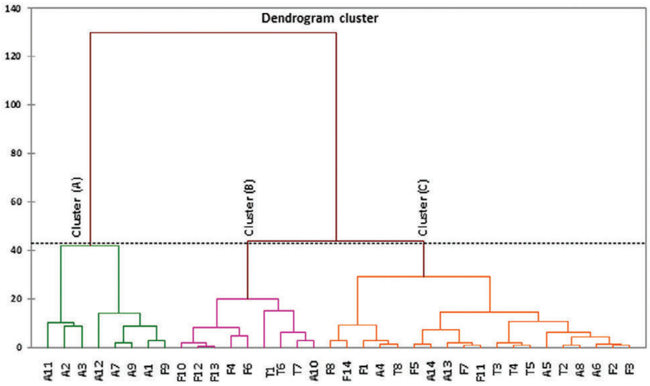


*Fig. 13 - Classification of the studied parameters and sources according to HCA.*

Fig. 13 - Classificazione dei parametri e delle fonti studiati secondo la HCA.

### *Water quality index (WQI)*

Water quality is main information in nature resources management (Abdelaziz et al., 2020). It presents the water parameter datas that aggregate to produce a single value of the water quality from the huge amount of variable (Nguyen et al., 2022). With other parameters such as hydrogeochemical facies study and pollution index evaluation, the water quality index remains the most important to determine the groundwater quality for drinking and irrigation (Aljanabi et al., 2021). So, water quality standards have been established to evaluate this index on international and regional scale.

According the established Box plot (Fig. 14), the values of WQI are between 89.8 (Frenda) and 281.8 (Ain Hedid).

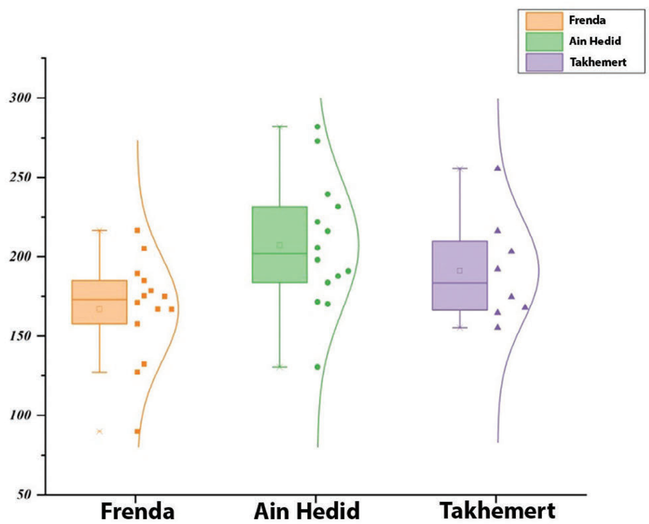


*Fig. 14 - Box plot of WQI.*

Fig. 14 - Box plot del WQI.

Additionally, the results showed that 2.7% of the samples from the studied alluvial plains belong to the good quality category (Table 5). While 63.8 % and 33.3% of the samples are classified in the poor and very Poor category respectively (Figure 15). Fortunately, our study disclosed a total absence of the very mediocre and unsafe drinking water categories.

*Tab. 5 - Water classification according to WQI (Nayak et al., 2022, Bekkoussa et al., 2018).*

Tab. 5 - Classificazione delle acque secondo il WQI (Nayak et al., 2022, Bekkoussa et al., 2018).

| Index Classes WQI | Sample numbers and (%) | |
|---|---|---|
| Excellent (<50) | None | |
| Good (50 – 100) | 1 | (2.7) |
| Poor (100 – 200) | 23 | (63.8) |
| Very poor (200 – 300) | 12 | (33.3) |
| Unsafe drinking water (>300) | None | |

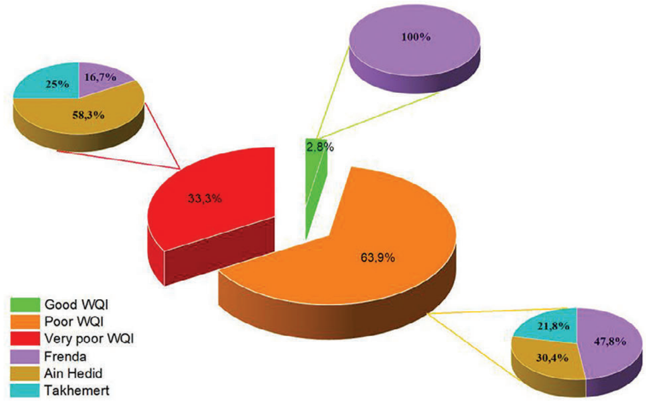


*Fig. 15 - Water quality index for the three studied regions.*

Fig. 15 - Indice di qualità dell'acqua per le tre regioni studiate.

According to the mapping and the special analysis of the WQI of the study region (Fig. 16), it has been shown that the whole region has poor to very poor potability, except the part of Frenda, with good potability (Agidi et al., 2022).

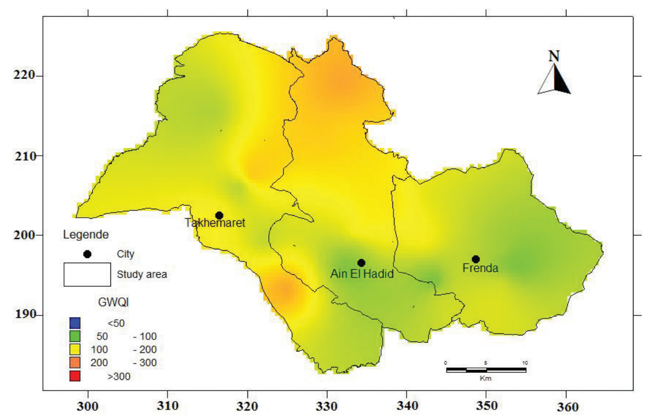


*Fig. 16 - Map of the water quality index.*

Fig. 16 - Mappa dell'indice di qualità dell'acqua.

### *Correlation between the water quality index and the major elements*

According to the studied correlations between WQI and the determined ions, the increase in the amounts of the cations affects negatively the final water quality. Nevertheless, the evaluated index decreases with high values of $HCO_3^-$. Upon studying the analysis correlation (Fig. 17), the water quality index is positively correlated with $Na^+$ ,$K^+$, $Mg^{2+}$, $Ca^{2+}$ , and $Cl^-$, $SO_4^{2-}$ ions (Zamiche et al., 2018). Results confirmed by the

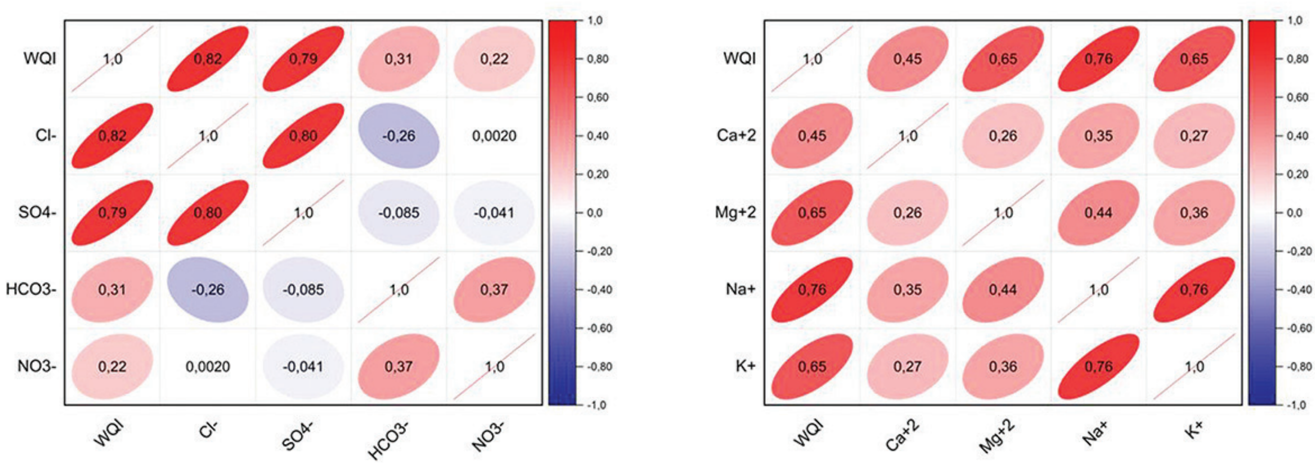


*Fig. 17 - Correlation between the water quality index and the major ions.*

Fig. 17 - Correlazione tra l'indice di qualità dell'acqua e gli ioni principali.

Gibbs diagram (Fig. 9) where the origin of the mineralization is largely due to the alteration and dissolution of the source rock, in particular the carbonate rocks (dolomite) and the evaporitic rocks (halite and selvine) (Zamiche et al., 2018). Therefore the decrease in the water qualaty index of the study area is hightly dependent on the increase in $Na^+$, $K^+$ and $Cl^-$, $SO_4^{2-}$ (Mammeri et al., 2023; Hosseininia & Hassanzadeh, 2023).

## Evaluation of Groundwater Suitability for Irrigation

From the irrigation standpoint, most of the analyzed wells present an acceptable quality according to the evaluated indices such as SAR, %Na and Kelley's Index. However, the presence of high salinity levels in some wells could restrict their use for irrigation. The Magnesium Hazard Index (MH) highlighted a risk associated in particular with a high concentration of magnesium, concerning more than 33.3% of the studied wells (Table 6).

*Tab. 6 - Classification of groundwater quality according to irrigation index.*

Tab. 6 - Classificazione della qualità delle acque sotterranee in base all'indice di irrigazione.

| Parameters | Range | Water class | Samples | Index percentage (%) |
|---|---|---|---|---|
| Alkalinity hazard (SAR) | <10 | Excellent | 36 | 100 |
| | 10 – 18 | Good | 0 | 0 |
| | 18 – 26 | Doubtful | 0 | 0 |
| | >26 | Unsuitable | 0 | 0 |
| Salinity hazard (EC) | <250 | Excellent | 0 | 0 |
| | 250 – 750 | Good | 04 | 11.11 |
| | 750 – 2000 | Permissible | 26 | 72.22 |
| | 2000 – 3000 | Doubtful | 03 | 8.33 |
| | >3000 | Unsuitable | 03 | 8.33 |
| Sodium percentage (Na %) | <20 | Excellent | 12 | 33.33 |
| | 20 – 40 | Good | 16 | 44.44 |
| | 40 – 60 | Permissible | 6 | 16.66 |
| | 60 – 80 | Doubtful | 2 | 5.55 |
| | >80 | Unsuitable | 0 | 0 |
| Kelly Index (KI) | <1.0 | Suitable | 33 | 91.66 |
| | >1.0 | Unsuitable | 03 | 8.33 |
| Magnesium Hazard (MH) % | <50 | Suitable | 24 | 66.66 |
| | >50 | Unsuitable | 12 | 33.33 |

## Conclusion

In this study, water quality index (WQI) has been assessed to characterize the suitability of groundwater of 36 samples throughout three regions in the plain of Tiaret (Northwestern Algeria). According to this study, the pH values of all the samples have alkaline properties. Indeed, Piper diagram shown three chemical facies. The first is bicarbonate calcium ($HCO_3$-Ca) and the second is chloride Sodium (Cl-Na) and the third one is bicarbonate magnesium ($HCO_3$-Mg). According to WHO (2008), $HCO_3^-$ and Cl- are the dominant anions, while $Ca^{2+}$ and $Mg^{2+}$ represent the majority cations.

The spatial distribution of ions reveals that calcium is widely present throughout the plain, while magnesium and sodium are mainly concentrated in the north and southwest of Ain Hedid, as well as at the center of Takhemert. $Cl^-$ and sulphate are primarily found in the northwestern part of Ain Hedid. Furthermore, this region and the center of Frenda, are characterized by high nitrate concentrations.

The results indicated that electrical conductivity (EC) and TDS are strongly correlated with most ions, except $HCO_3^-$ and $NO_3^-$, while pH exhibited a weaker correlation with the other elements. A positive correlation was also found between $Na^+$ and the anions $Cl^-$, $SO_4^{2-}$ and $K^+$. Additionally, a positive correlation is observed between $Cl^-$ and $K^+$, $SO_4^{2-}$ and $Mg^{2+}$.

Gibbs diagram confirmed that evaporation and mineral weathering are the main factors affecting the chemical composition of studied groundwater. Indeed, The Durov diagram revealed that most water samples exhibited simple dissolution or mixing.

According to the statistical analysis, most of the parameters (EC, $Na^+$, $Cl^-$, $K^+$, and $SO_4^{2-}$) are associated with PC1, indicating that mineralization process is mainly caused by salinization. The second factor, PC2, is strongly correlated with pH and T°C, suggesting that temperature increases may influence the rate of chemical reactions, potentially raising the pH of the water. The final factor, PC3, is correlated with nitrate and bicarbonate, which are key indicators of contamination linked to agricultural activities. The HCA method revealed three clusters upon analysis.

The results of the WQI showed that 2.7%, 63.8 % and 33.3% of the samples belong to the good quality category, poor and very poor category respectively. Most of the analyzed wells meet acceptable groundwater quality standards for irrigation, based on indices such as SAR, Na%, and Kelley's Index. However, high salinity levels in some wells may limit their use for irrigation. The Magnesium Hazard Index (MH) identified a risk, particularly due to high magnesium concentrations, affecting more than 33.3% of the studied wells.Therefore, this study recommends that the groundwater in this region be preserved and protected to ensure sustainable development. Moreover and as perspective, a future research will focus on isotopic analyses to enhance understanding of groundwater origin and recharge mechanisms in this area.

### Competing interest

The authors declare no competing interest.

### Acknowledgments

We would like to thank ZEMOUR Hafidh and CHERIER Hamid (Algeria) for their contribution in this work.

### Author contributions

ATEA, MB, BBS, ZK and MM carried out laboratory work and analysed data. ATEA, MB and BBS advised about the laboratory technique and conducted manuscript proofreading before submission. All authors read and approved the final version of the manuscript.

### Funding source

The authors declare no founding source

### Additional information

**DOI:** https://doi.org/10.7343/as-2025-852

**Reprint and permission information** are available writing to acquesotterranee@anipapozzi.it

**Publisher's note** Associazione Acque Sotterranee remains neutral with regard to jurisdictional claims in published maps and institutional affiliations.

## REFERENCES

Abdelaziz, S., Gad, M.I., & El Tahan, A. H. M. H. (2020). Groundwater quality index based on PCA: Wadi El-Natrun, Egypt. Journal of African Earth Sciences.172, 103964. https://doi.org/10.1016/j.jafrearsci.2020.103964

Adimalla, N., & Qian, H. (2021). Groundwater chemistry, distribution and potential health risk appraisal of nitrate enriched groundwater: A case study from the semi-urban region of South India. Ecotoxicology and Environmental Safety, 207, 111277. https://doi.org/10.1016/j.ecoenv.2020.111277

Adimalla, N. (2019). Controlling factors and mechanism of groundwater quality variation in semiarid region of South India: an approach of water quality index (WQI) and health risk assessment (HRA). Environmental Geochemistry and Health, 42, 1725–1752. https://doi.org/10.1007/s10653-019-00374-8

Agidi, B. M., Akakuru, O. C., Aigbadon, G. O., Schoeneich, K., Isreal, H., Ofoh., I., Njoku., J., & Esomonu, I. (2022). Water quality index, hydrogeochemical facies and pollution index of groundwater around Middle Benue Trough, Nigeria. International Journal of Energy and Water Resources, 8(1), 35-54. https://doi.org/10.1007/s42108-022-00187-z

Aljanabi, Z. Z., Al-Obaidy, A. H. M. J., & Hassan, F. M. (2021). A brief review of water quality indices and their applications. IOP Conference Series: Earth and Environmental Science.779, 012088. 10.1088/1755-1315/779/1/012088

Amadou, S., Seyni, N., & Serigne, F. (2022). Hydrogeochemical characterization of the Samba Dia aquifer (Central West Senegal). International Journal of Innovation and Applied Studies, 38(1), 71-85.

Ameur, M., Hamzaoui-Azaza, F., & Gueddari, M. (2016). Nitrate contamination of Sminja aquifer groundwater in Zaghouan, northeast Tunisia: WQI and GIS assessments. Desalination and Water Treatment, 57(50), 23698–23708. https://doi.org/10.1080/19443994.2015.1137495

Barakat, A. (2020). Groundwater $NO_3$ concentration and its potential health effects in Beni Moussa perimeter (Tadla plain, Morocco). Geoenviron Disasters, 7, 14. https://doi.org/10.1186/s40677-020-00149-9

Batarseh, M., Imreizeeq, E., Tilev, S., Al Alaween, M., Suleiman, W., Al Remeithi, A. M., Al Tamimi, M. K., & Al Alawneh, M. (2021). Assessment of groundwater quality for irrigation in the arid regions using irrigation water quality index (IWQI) and GIS-Zoning maps: case study from Abu Dhabi Emirate, UAE. Groundwater for Sustainable Development, 14, 100611. https://doi.org/10.1016/j.gsd.2021.100611

Bekkoussa, B., Bekkoussa, S., Taupin, J. D., Patris, N., & Azzaz, H. (2017). Mapping of the Groundwater Quality Index of the Ghriss Plain, North-West Algeria. Water Resources and Climate Change Anthropic and Climatic Impacts on the Variability of Water Resources,1-6.

Bekkoussa, S., Bekkoussa, B., Taupin, J. D., Patris, N., & Meddi, M. (2018). Groundwater hydrochemical characterization and quality assessment in the Ghriss Plain basin, northwest Algeria. Journal of Water Supply Research and Technology-Aqua, 67 (5), 458-466. https://doi.org/10.2166/aqua.2018.013

Benadela, L., Bekkoussa, B., & Gaidi, L. (2022). Multivariate analysis and geochemical investigations of groundwater in a semi-arid region, case of superficial aquifer in Ghriss Basin, Northwest Algeria. Journal of Groundwater Science and Engineering, 10(3), 233-249. https://doi.org/10.19637/j.cnki.2305-7068.2022.03.003

Bitencourt, E. B., Almeida, K. M., Santos, L. M. M., & Júnior, A. P. (2019). Physicochemical and microbiological characterization of the influence of waste on the water quality of the Tocantins River, left bank (MARAB-PA). Revista Científica Multidisciplinar Núcleo do Conhecimento, 11, 05-26.

Brown, R. M., McClelland, N. I., Deininger, R. A., & O'Connor, M. F. (1972). A Water Quality Index-Crashing the Psychological Barrier. In: Thomas, W.A. (eds) Indicators of Environmental Quality. Environmental Science Research, 1. 173–182. https://doi.org/10.1007/978-1-4684-2856-8_15

Brown, R. M., McClelland, N. I., Deininger, R. A., & Tozer, R. G.(1970). A Water Quality Index- Do We Dare? Water and Sewage Works, 117, 339-343.

Calligaris, C., Ghezzi, L., Petrini, R., Lenaz, D., & Zini, L. (2019). Evaporite Dissolution Rate through an on-site Experiment into Piezometric Tubes Applied to the Real Case-Study of Quinis (NE Italy). Geosciences, 9(7), 298. https://doi.org/10.3390/geosciences9070298

Chadli, K., & Boufala, M. (2021). Assessment of water quality using Moroccan WQI and multivariate statistics in the Sebou watershed (Morocco). Arabian Journal of Geosciences, 14, 27. https://doi.org/10.1007/s12517-020-06296-5

Chen, C., Hanting, Z., Xinyu, W., Meng, N., Xia, W., Yuzhu, G., Han, W., Ruifeng, T., & Mingcai, H. (2023). Thermodynamic and Kinetic Studies of Dolomite Formation: A Review. Minerals, 13 (12), 1479. https://doi.org/10.3390/min13121479

Chen, J., Qian, H., Gao, Y., Wang, H., & Zhang, M. (2020). Insights into hydrological and hydrochemical processes in response to water replenishment for lakes in arid regions. Journal of Hydrology. 581, 124386. https://doi.org/10.1016/j.jhydrol.2019.124386

Cosgrove, S., Jefferson, B., & Jarvis, P. (2019). Pesticide removal from drinking water sources by adsorption: a review. Environmental Technology Reviews, 8(1), 1-24. https://doi.org/10.1080/21622515.2019.1593514

Durov, S. A. (1948). Classification of Natural Waters and Graphical Representation of Their Composition. Doklady Akademii Nauk SSSR, 59, 87-90.

El Baba, M., Kayastha, P., Huysmans, M., & De Smedt, F. (2020). Evaluation of the Groundwater Quality Using the Water Quality Index and Geostatistical Analysis in the Dier al-Balah Governorate, Gaza Strip, Palestine. Water, 12(1), 262. https://doi.org/10.3390/w12010262

Fartas, F., Reminib, B., Sekiou, F., & Marouf, N. (2022). The use of PCA and ANN to improve evaluation of the WQIclassic, development of a new index, and prediction of WQI, Coastel Constantinois, northern coast of eastern Algeria. Water Supply, 22 (12), 8727–8749. https://doi.org/10.2166/ws.2022.389

Fu, T., Qi, C., Wang, Z., Li, C., Liu, W., Fu, Y., Chen, G., Su, Q., Xu, X., & Yu, H. (2022). Hydrochemical Characteristics and Quality Assessment of Groundwater under the Impact of Seawater Intrusion and Anthropogenic Activity in the Coastal Areas of Zhejiang and Fujian Provinces, China. Lithosphere, 18, 1394857. https://doi.org/10.2113/2022/1394857

Galal Uddin, M. d., Moniruzzaman, M. d., Abdul Quader, M., & Abu Hasan, M. d. (2018). Spatial variability in the distribution of trace metals in groundwater around the Rooppur nuclear power plant in Ishwardi, Bangladesh. Groundwater for Sustainable Development, 7, 220-231. https://doi.org/10.1016/j.gsd.2018.06.002

Galal Uddin, M. d., Nash, S., & Olbert, A. I. (2021). A review of water quality index models and their use for assessing surface water quality. Ecological Indicators, 122, 107218. https://doi.org/10.1016/j.ecolind.2020.107218

Gan, S., Zhang, M., Yu, K., Zhou, Y., & Yan, B. (2022). Groundwater quality assessment using principal component analysis modified water quality index in the Huangbizhuang, Northern China Plain. Human and Ecological Risk Assessment: An International Journal, 29(2), 597–620. https://doi.org/10.1080/10807039.2022.2154193

Gaur, N., Sarkar, A., Dutta, D., Gogoi, B. J., Dubey, R., & Dwivedi, S. K. (2022). Evaluation of water quality index and geochemical characteristics of surfacewater from Tawang India. Scientific Reports,12(1), 11698. https://doi.org/10.1038/s41598-022-14760-3

Gibbs, R. J. (1970). Mechanisms controlling world water chemistry. Science, 170(3962), 1088–1090.

Hosseininia, M., & Hassanzadeh, R. (2023). Groundwater quality assessment for domestic and agricultural purposes using GIS, hydrochemical facies and water quality indices: case study of Rafsanjan plain, Kerman province, Iran. Applied Water Science, 13, 84 https://doi.org/10.1007/s13201-023-01891-9

Jasechko, S., Perrone, D., Befus, K. M., Bayani Cardenas, M., Ferguson, G., Gleeson, T., Luijendijk, E., McDonnell, J. J, Taylor, R. G., Wada, Y., & Kirchner, J. W. (2017). Global aquifers dominated by fossil groundwaters but wells vulnerable to modern contamination. Nature Geoscience, 10(6), 425-429. https://doi.org/10.1038/ngeo2943

Kelly, W. P. (1963). Use of Saline Irrigation Water. Soil Science, 95, 385-391. https://doi.org/10.1097/00010694-196306000-00003

Kenniche, S., Bekkoussa, B., M'nassri, S., Teffahi, M., Taupin, J. d., Patris, N., Zaagane, M., & Majdoub, R. (2022). Hydrochemical characterization, physicochemical and bacteriological quality of groundwater in Sidi Kada Mountains, northwest of Algeria. Arabian Journal of Geosciences, 15, 1061. https://doi.org/10.1007/s12517-022-10298-w

Kom, K. P., Gurugnanam, B., Bairavi, S., & Chidambaram, S. (2023). Sources and geochemistry of high fluoride groundwater in hard rock aquifer of the semi-arid region. A special focus on human health risk assessment. Total Environment Research Themes. 5, 100026. https://doi.org/10.1016/j.totert.2023.100026

Li, Y., & Li, X. (2021). Research on water distribution systems from the past to the future: a bibliometric review. Environmental Technology Reviews, 10(1), 161–176. https://doi.org/10.1080/21622515.2021.1900404

Liun, C. W, Linn, K. H., & Kuon, Y. M. (2003). Application of factor analysis in the assessment of groundwater quality in a black foot disease area in Taiwan. Science of the Total Environment, 313(1–3), 77–89. https://doi.org/10.1016/S0048-9697(02)00683-6

Lloyd, J. W., & Heathcoat, J. A. (1985). Natural Inorganic Chemistry in Relation to Groundwater. Clarendon Press, Oxford.

Mammeri, A., Tiri, A., Belkhiri, L., Salhi, H., Brella, D., Lakouas, E., Tahraoui, H., Amrane, A., & Mouni, L. (2023). Assessment of Surface Water Quality Using Water Quality Index and Discriminant Analysis Method. Water, 15(4), 680. https://doi.org/10.3390/w15040680

Martínez-Martínez, J., Anna, A., & David, B. (2021). The Role of Calcite Dissolution and Halite Thermal Expansion as Secondary Salt Weathering Mechanisms of Calcite-Bearing Rocks in Marine Environments. Minerals, 11(8), 911. https://doi.org/10.3390/min11080911

Mehreen, A., Rafia, M., & Syed Mohammad, H. Z. (2021). Analysis of water quality indices and machine learning techniques for rating water pollution: a case study of Rawal Dam, Pakistan. Water Science and Technology Water Supply, 21(4), 3225.3250. https://doi.org/10.2166/ws.2021.082

Misaghi, F., Delgosha, F., Razzaghmanesh, M., & Myers, B. (2017). Introducing a water quality index for assessing water for irrigation purposes: A case study of the Ghezel Ozan River. Science of The Total Environment, 589 , 107–116. https://doi.org/10.1016/j.scitotenv.2017.02.226

Nayak, A., Matta, G., & Uniyal, D. P. (2022). Hydrochemical characterization of groundwater quality using chemometric analysis and water quality indices in the foothills of Himalayas. Environment, Development and Sustainability, 13, 1-32. 10.1007/s10668-022-02661-4

Nguyen, V. H., Nguyen, V. H., Truong, T. K., Nguyen, H. P., & Nguyen, D. G. C. (2022). A comprehensive procedure to develop water quality index: A case study to the Huong river in Thua Thien Hue province, Central Vietnam. PLoS ONE, 17(9), e0274673.
https://doi.org/10.1371/journal.pone.0274673

Ragunath, H. M. (1987). Groundwater. Wiley Eastern Ltd., New Delhi, 563.

Rahal, O., Layachi, G., Garrote, L. Sappa, G., Balacco, G., Brahmi, S., & Maria de Filippi, F. (2024). Assessing the Impact of Climate Variability and Human Activity on Groundwater Resources in the Meskiana Plain, Northeast Algeria. Water Resources, 51, 1042–1053 . https://doi.org/10.1134/S0097807824603406

Rahman, K., Barua, S., & Imran, H. M. (2021). Assessment of water quality and apportionment of pollution sources of an urban lake using multivariate statistical analysis. Cleaner Engineering and Technology, 5, 100309. https://doi.org/10.1016/j.clet.2021.100309

Richards, L. A. (1954). Diagnosis and Improvement of Saline and Alkali Soils, Hand Book, 60. U.S. Department of Agriculture, Washington D.C.

Rodier, J., Legube, B., Merlet, N., & Brunet, R. (2009). Water analysis: natural waters, waste water, sea water. 8th edition. Dunod. Paris, France. 1579p

Safa, A. (2010). Contribution to the hydrogeological study of the Mina watershed, arid to semi-arid zone (Hautes Plaines Oranaises, north-western Algeria). PhD Thesis. Oran University.Algeria. 207p.

Sharma, S., Kaur, I., & Nagpal, A. K. (2017). Assessment of arsenic content in soil, rice grains and groundwater and associated health risks in human population from Ropar wetland, India, and its vicinity. Environmental Science and Pollution Research, 24(23), 18836–18848. 10.1007/s11356-017-9401-y

Strojexport (1976). Geophysical study of the alluvial plains of Oueds el Abd and el Taht. 70p.

Vasanthavigar, M., Srinivasamoorthy, K., Vijayaragavan, K., Rajiv Ganthi, R., Chidambaram, S., Anandhan, P., Manivannan, R., & Vasudevan, S. (2010). Application of water quality index for groundwater quality assessment: Thirumanimuttar sub-basin, Tamilnadu, India. Environmental Monitoring and Assessment, 171, 595-609. https://doi.org/10.1007/s10661-009-1302-1

Wątor, K., & Zdechlik, R. (2021). Application of water quality indices to the assessment of the effect of geothermal water discharge on river water quality- a case study from the Podhale region (Southern Poland). Ecological Indicators, 121, 107098. https://doi.org/10.1016/j.ecolind.2020.107098

WHO. (2008). Guidelines for drinking-water quality, World Health Organization, Geneva, Switzerland, 3rd edition,

Wilcox, L. (1955). Classification and uses of irrigation waters. USDA Circular No. 969, Washington, DC.

Yahiaoui, S., Meddi, M., Razack, M., Boufekane, A., & Bekkoussa, B. S. (2023). Hydrogeochemical and isotopic assessment for characterizing groundwater quality in the Mitidja plain (northern Algeria). Environmental Science and Pollution Research, 30, 80029–80054. https://doi.org/10.1007/s11356-023-27952-9

Zamiche. S., Hamaidi-Chergui, F., & Demiai, A. (2018). Pollution of the quaternary aquifer of Mitidja (Algeria) by nitrates: Origins and impacts on the quality of water for human consumption. Journal of Fundamental and Applied Sciences, 10(1), 113. 10.4314/jfas.v10i1.8

Zemour, Y., Mebrouk, N., Mayer, A., Mekebret, I., & Sherif, M. I. (2023). Hydrochemical and geological controls on dissolved radium and radon in northwestern Algeria hydrothermal groundwaters. Chemosphere,313.137573.https://doi.org/10.1016/j.chemosphere.2022.13757